1 **Different responses of the trophic features of particulate organic matter to summer constraints in the**

2 **Ross Sea**

3

4 Cristina Misic[1], Anabella Covazzi Harriague[1] , Olga Mangoni [2],

5 Yuri Cotroneo[3], Giuseppe Aulicino[3], Pasquale Castagno[3]

6

7 [1] Dipartimento di Scienze della Terra, dell'Ambiente e della Vita – University of Genova, C.so Europa 26, 16132 Genova, Italy

8 [2] Dipartimento di Biologia, University of Napoli Federico II, Via Mezzocannone, 8, 80134 Napoli, Italy.

9 [3] Dipartimento di Scienze e Tecnologie, University of Napoli Parthenope, Centro Direzionale di Napoli IS. C4, 80143 Napoli, Italy

10

11

12

13

14 Corresponding author:

15 Cristina Misic, Dipartimento di Scienze della Terra, dell'Ambiente e della Vita - University of Genova

16 C.so Europa 26, 16132 Genova, Italy.

17 Phone: +3901035338224, e-mail: misic@dipteris.unige.it

Abstract

The 0-200 m surface layer of the Ross Sea was studied during summer 2014 to highlight the trophic features of the particulate organic matter (POM) in specific areas. With the aid of satellite information, we selected three zones, characterised by different distances from the coast and different mesoscale hydrodynamic structures: a northern offshore area, crossing the summer-polynya area of the Ross Sea (hereafter called ROME 1), a more coastal area next to the Terra Nova Bay polynya (ROME 2); a southern offshore area, towards the Ross Ice Shelf (ROME 3). Ice-maps showed that the ice retreat had already occurred, leaving general open-water conditions. The statistical analysis of the quantitative features (organic carbon, nitrogen, protein and carbohydrate concentrations) and qualitative trophic characteristics (lability to consumption and caloric value) of the POM pointed to significant differences between the stations, especially in the upper mixed layer (UML). A comparison with other studies previously carried out in the same areas showed that the localised pulses of the POM accumulation in the UML were similar to those recorded at the highly productive marginal ice zones. Therefore, the summer processes could provide significant quantities of materials and energy to the ecosystem, likely also sustaining it in autumn and winter. The UML layer, rather thin and easily subjected to alterations due to global climate change, confirmed its pivotal role in the ecosystem dynamics. A good POM trophic quality was highlighted at several stations in ROME 1 and ROME 3. Reduced trophic support was, instead, found in ROME 2. A proportionally reduced POM consumption in this area, where deep-water formation takes place, would increase the relevance of the POM in the transfer of C to the depths.

1. Introduction

Particulate organic matter (POM) is composed of a variety of macromolecules and aggregates, whose dimension ranges, arbitrarily, between 0.45-1 μm and 200 μm. POM hosts detrital matter as well as living organisms. Ice-algae, phytoplankton, nano- and microzooplancton, and mesozooplancton-derived particles are included in POM. The presence of phytoplanktonic organisms inside the POM necessitates that its primary ecological role is the foraging of the trophic web in the open sea, where benthic primary production does not occur. On the other hand, the detrital and the heterotrophic microbial components of the POM highlight the fact that this dimensional fraction also has a role in recycling the elements. In addition, POM enters the fluxes of C to the deep waters, taking part to the biological pump that regulates C concentrations in the hydrosphere and atmosphere (Fonda Umani et al., 2002).

In the Antarctic Ocean the quantitative features of the POM have been extensively studied (especially chlorophyll-a, particulate organic carbon - POC - and particulate nitrogen - PN) (Smith et al., 2000; Smith and Asper, 2001), while detailed information on its trophic features is rather scarce. The trophic quality of POM may be studied by means of proxies of its nutritional value. The ratios that are commonly used to infer the trophic value of the POM (for instance the POC/PN ratio and the POC/chlorophyll-a ratio) may be implemented by analyses focusing on its caloric content and on the hydrolysable fractions of the POM (Fabiano et al. 1993; Fabiano and Pusceddu, 1998; Misic and Covazzi Harriague, 2008; Kim et al., 2014). The caloric content expresses the actual value of the POM in energy terms. In this case, different biochemical features generate quantitatively different trophic values for the POM. For the hydrolysable fraction, biomimetic assays have been developed to evaluate the fraction that may be rapidly hydrolysed by the enzymes commonly found in the environment, to calculate the actual fraction of the POM that is bioavailable to consumers. This approach by-passes the uncertainty of bulk-related analyses (such as POC). In fact, the chemical form of the food supply achieves a high relevance for an efficient biological exploitation. The biomimetic assay allows for the possibility that some compounds may be biochemically refractory to consumption, or physically enclosed in low-lability materials that isolate them from consumers.

Interannual, seasonal and spatial variability of biological features is typical of the Antarctic Ocean and the Ross Sea (Smith et al., 1996; Arrigo et al., 1998; Dunbar et al., 1998; Gardner et al., 2000; Fragoso and Smith, 2012). However, the mechanisms forcing this spatial heterogeneity are still largely unclear. The presence of ice regulates the onset of primary production, POM accumulation and fluxes in the water column (Garrity et al., 2005). The ice-associated processes physically influence the water column, determining the depth of the upper mixed layer (UML) that is often considered to be a major factor in controlling POM production and distribution (Fragoso and Smith, 2012). Therefore, general trends may be highlighted, based on the degree of maturity of the selected system (Fabiano et al., 2000): closed pack conditions, followed by the Marginal Ice Zone (MIZ) spring conditions, and then by open waters in late spring and summer, generally in the offshore area by late December and in the entire continental shelf region by late January (Comiso et al., 1993, Smith and Asper, 2001). Knowing that ice regulates the biological development and, consequently, the features of the POM, other forces must influence the planktonic patterns when ice is lacking, during summer for instance. Although ice may last longer at some sites in the Ross Sea, depending on global climate anomalies as well as local events (Arrigo and van Djiken, 2004), the summer features of the Ross Sea should show less variability than the spring ones. The stratification generated by ice melting should be relaxed due to wind and waves on the open waters, a feature that would allow increased vertical fluxes and a more homogeneous vertical distribution of the POM (Gardner et al., 2000).

This study is based on the results of the ROME (Ross Sea Mesoscale Experiment) cruise, carried out during the Antarctic summer of 2014. Sampling was performed focusing on the 0-200 m surface layer of three areas of the Ross Sea, characterised by different distances from the coast and different mesoscale hydrodynamic structures.

We aimed to: i) highlight whether the quantitative and qualitative features of the POM were homogeneous in the sampled areas, ii) test whether our summer POM features resembled those of previous research performed in the Ross Sea, iii) underline the potential role of the POM in the trophic exchanges and in the global carbon trends of the area.

92

2. Material and methods

2.1 Station sites and sampling

The in situ ROME data were collected by the R/V Italica in the framework of the Italian National Program for

Antarctic Research (PNRA). Sampling was performed in three different areas of the Ross Sea: ROME 1 was

sited at approximately 170°E and 75°S; ROME 2 occupied a more coastward area, next to the Terra Nova

Bay (TNB) polynya; ROME 3 was sited in the southern Ross Sea, towards the Ross Ice Shelf, at 168°E (Fig.

1A).

The sampling strategy was defined on the basis of the MODIS (Moderate Resolution Imaging

Spectroradiometer) Aqua and Terra satellite level-2 products for the previous 12/24 hours. In particular,

the sea surface temperature and surface chlorophyll-a concentration maps at 1 km resolution were

analyzed in order to plan and to carry out the casts in correspondence with both high and low chlorophyll

signals. Additionally, satellite AMSR2 sea ice concentration maps, provided by the University of Bremen,

using the ASI sea ice concentration algorithm (Spreen et al., 2008), were considered. In fact, daily maps of

the Ross Sea region from early December 2013 to late February 2014 (available at http://www.iup.uni-

bremen.de:8084/amsr2) were analyzed to monitor the evolution of the sea ice cover before and during the

experiment, in order to study its effects on the physical and biochemical systems.

A total of 46 casts were obtained. Hydrological profiles were acquired by means of a SBE 9/11 Plus CTD,

with double temperature and conductivity sensors. For each station the upper mixed layer (UML) depth

was determined as the depth at which *in situ* density (σ_t) changed by 0.05 kg/m^3 over a 5 m depth interval.

Current speed and direction were recorded using a Lowered Acoustic Doppler Current Profiler (LADCP)

system. Two LADCP were deployed with a CTD, to obtain a unique current measurement every 10 m from

the surface to the maximum depth reached. The effect of tides on this current dataset was removed

following the procedure proposed by Erofeeva et al. (2005).

The POM sampling was performed at 21 stations (Table 1, black circled stations in Fig. 1A) using 12-L

Niskin bottles. Samples were collected at 4 fixed depths (surface, 50, 100 and 200 m) and 1 variable depth

118   depending on the maximum of the signal for fluorescence. From 0.5 to 1 L of sampled seawater was filtered

119   through Whatman GF/F filters (nominal pore diameter 0.7 µm), and immediately frozen until analysis in the

120   laboratory.

121

122   *2.2 Analytical procedures*

123   The filters for the spectrofluorometric analyses of the chlorophyll-a and phaeopigments were stored at −

124   80°C and analyzed with a Varian Eclipse spectrofluorometer, following Holm Hansen et al. (1965). The

125   instrument was checked daily with a chlorophyll-a standard solution (from *Anacystis nidulans* by Sigma).

126   The specific standard deviation of the replicates was on average 4%.

127   Particulate organic carbon (POC) and particulate nitrogen (PN) were analyzed following Hedges and Stern

128   (1984), after acidification with HCl fumes in order to remove inorganic carbon. Cyclohexanone 2-4-

129   dinitrophenyl hydrazone was used to calibrate a Carlo Erba Mod. 1110 CHN Elemental Analyser. The

130   specific standard deviations due to the analytical procedures and sample handling were 7.4% and 7.8% for

131   POC and PN, respectively.

132   Particulate proteins, particulate carbohydrates and particulate lipids were analyzed following Hartree

133   (1972), Dubois et al. (1956), Bligh and Dyer (1959) and Marsh and Weinstein (1966). Albumin, glucose and

134   tripalmitine solutions were used to calibrate a Jasco V530 spectrophotometer. The specific standard

135   deviations were 8.3%, 15.5% and 21.6% for the proteins, carbohydrates and lipids, respectively.

136   Besides the quantitative information given by the single concentration of the different elements and

137   biochemical types, the POC/PN ratio (Huston and Deming, 2002) and the particulate protein/carbohydrate

138   ratio (Misic and Fabiano, 1996) gave clues to the qualitative value of the POM for the consumer. The lower

139   the POC/PN and the higher the protein/carbohydrate ratio, the higher the trophic value of the POM.

140   The concentrations of proteins, carbohydrates and lipids were used to calculate the caloric value of the

141   POM (Kcal g POM^{-1}) following the Winberg (1971) equation (Kcal g POM^{-1} = 0.055 protein% +0.041

142   carbohydrate% + 0.095 lipid%).

143   The hydrolysable particulate proteins and carbohydrates were determined following the protocols of

144   Gordon (1970), Mayer et al. (1995) and Dell'Anno et al. (2000). The sample filters and filter blanks

145   (Whatman GF/F filters not used for filtration) were placed in plastic containers with solutions (100 mg l^{-1} in

146   0.1 M Na-phosphate buffer) of two selected enzymes purchased from Sigma–Aldrich. Proteinase K was

147   chosen for the hydrolysis of the proteins, β-glucosidase for that of the carbohydrates. These enzymes are

148   extracted from plants and fungi, but have hydrolytic activities quite similar to natural marine organisms and

149   are widespread among autotrophs and heterotrophs (Dall and Moriarty, 1983). The filters were left in the

150   enzyme solutions for 2 hours, at the optimal temperatures and pH for each enzyme in order to enhance the

151   digestion. After hydrolysis, each filter was carefully removed from its container, placed in a filter-holder and

152   rinsed with the solution remaining in the dish and 5ml of deionised water to return any particles that may

153   have floated off the filter. Then the filters were processed for the determinations of proteins and

154   carbohydrates following the same protocols as above. The possibility that the flushing of the buffer could

155   have mechanically removed part of the particulate fraction was avoided by incubating and processing

156   replicates of the samples with only the buffer solution. The concentrations detected after hydrolysis,

157   corrected for the eventual error just mentioned (never higher than 20% of the total protein and

158   carbohydrate concentrations), were subtracted from the total concentrations in order to obtain the

159   hydrolysable, or labile, POM. The specific standard deviations were 11.2% and 21.5% for hydrolysable

160   particulate proteins and carbohydrates, respectively.

161

162   *2.3 Data treatment and statistical analysis*

163   The data were divided into a surface layer and a deeper layer, the former defined by the UML depth (Table

164   1) and the latter ranging from the UML depth down to 200 m.

165   The literature data related to previous research carried out in the Ross Sea and TNB were utilised as a

166   comparison. For the Ross Sea Fabiano et al. (2000) provided spring data and Fabiano et al. (1993) and

167   Catalano et al. (1997) early summer data. Fabiano et al. (1995 and 1997) and Povero et al. (2001) provided

168   summer data for the TNB area (Table 2).

169 We tested the differences of the same variable between different samplings with the one-way ANOVA test

170 followed by the Newman-Kneuls *post-hoc* test (ANOVA-NK test) (Statistica software). To test the

171 relationships between the various parameters, a Spearman-rank correlation analysis was performed.

172 The Principal Component Analysis (PCA) was applied to the normalised data of the POC, protein and

173 carbohydrate concentrations and the protein/carbohydrate ratio (PRIMER software). The data were divided

174 into the UML and the deeper layer, as previously described. The ROME data were treated together with the

175 other literature data previously cited (Table 2) to highlight similarities between them. The analysis of

176 similarities (ANOSIM) was applied to highlight significant differences between the groups identified by the

177 cluster analysis performed on the normalised data (resemblance measure: Euclidean distances, cluster

178 mode: group average), while the similarity percentage analysis (SIMPER) was utilised to highlight the

179 parameters responsible for such differences.

180

181 **3. Results**

182 *3.1 Physical properties and sea-ice conditions*

183 The Θ/S diagram obtained from all the sampled stations (Fig. 1B) indicated the presence of several typical

184 Ross Sea shelf water masses. In all the areas studied the surface layer was occupied by the Antarctic

185 Surface Water (AASW), a relatively light surface water characterized by potential temperatures ranging

186 between -1.8°C and +1°C and by salinity values lower than 34.50 (Orsi and Wiederwohl, 2009). According to

187 previous studies (Orsi et al., 2009), a westward increase in salinity was evident in this layer. In ROME 2 (blue

188 circles in Fig. 1B), the AASW core was slightly saltier, colder and denser than expected, with salinity close to

189 34.60 and potential density lower than 27.9 kg/m^3. These values were similar to the Modified Circumpolar

190 Deep Water (MCDW) features, but the high oxygen concentration values (Rivaro et al., this issue) confirmed

191 that we were in the presence of a local AASW. Moreover, both in ROME 1 and ROME 2, isolated high

192 temperature values (> 1°C) were episodically observed in the first 35 m depth, probably due to summer

193 insulation.

194 The intermediate and deep layers (from 150 to 1000 m) were occupied by High Salinity Shelf Water (HSSW),

195 and by Terra Nova Bay Ice Shelf Water (TISW), the latter identified only in ROME 2 (Fig. 1B). HSSW is

196 characterized by salinity greater than 34.70, potential temperature near freezing point and potential

197 density greater than 27.9 kg/m^3 (Budillon et al., 2003; Rivaro et al., 2014). TISW is a local expression of the

198 typical ISW, characterized by potential temperatures below freezing point and salinity values of about

199 34.70 (Budillon and Spezie, 2000). It was located in the 150-350 m layer and was the coldest water mass

200 identified during the experiment.

201 The physical properties of the upper layer may also be linked to sea ice evolution in the study area. The ice

202 melting in the Ross Sea gradually generates large ice-free areas during summer. Some ROME 1 and ROME 3

203 stations and all the ROME 2 stations experienced ice-free conditions starting from early December (Figs. 2A

204 and 2B). On the other hand, some stations experienced the presence of ice longer (Figs. 2C and 2D). Even in

205 the same sampling area, differences in ice cover can be significant and have an impact on the observed

206 temperature and salinity values. For instance, the northernmost station of ROME 1 (station 20) was

207 covered by ice until 14 January, just 3 days before the sampling. Stations 16 and 18 began to become ice-

208 free from the beginning of January (Fig. 2C). The ROME 3 stations were partially covered by ice until the

209 end of December, namely by the ice barrier lying between the Ross Sea summer polynya and the Ross

210 Island coastal opening (Fig. 2B).

211 The vertical structure of the water column of ROME 1 showed deeper UMLs for the stations that

212 experienced longer ice-free conditions (9, 11 and 13, Table 1). In the western stations of ROME 1 the lower

213 depth of the mixed layer depended on the presence of low-salinity surface water, related to the influence

214 of the ice (Fig. 3B). Intensity and direction of the currents in the UML (Fig. 3D) showed the presence of a

215 northward current along the eastern and western boundary of the leg, while more intense southward

216 velocities were registered in the central part of the leg (stations 13 and 14). This pattern was confirmed for

217 the entire water column (not shown).

218 The ROME 2 water column presented some peculiar features. The surface layer was characterized by a

219 temperature and salinity gradient between the fresher and colder coastal stations and the easternmost,

9

220   saltier and warmer stations (Figs. 4B and 4C). These hydrographical conditions limited the UML depth to

221   the first 10-15 m for all the sampled sites except stations 33 and 39, which had a slightly deeper UML (Table

222   1). A frontal structure was visible in the area between stations 45 and 34, where the convergence of the

223   two water masses led to a deepening of the thermocline down to 100 m (Rivaro et al., this issue). Stations

224   33 and 39 were separated from the coast by the front and showed features more similar to the offshore

225   stations. The differences between the coastal and offshore waters were also evident in the current pattern,

226   which made an abrupt change in direction along the frontal area, where intense southward velocities were

227   registered (Fig. 4D).

228   The strongest current intensities (p<0.05) were observed in ROME 3, with values up to 24 cm sec^{-1} for the

229   zonal (u) and meridional (v) components. The current pattern at all depths showed the presence of a

230   cyclonic circulation centred at about 168.5°E 76.45°S (Fig. 5D). This circulation could have increased the

231   UML water mixing, leading to salinity values of 34.23-34.43 and mean temperature values lower than 0.5°C

232   (Figs. 5B and 5C). In fact, the western and central stations (48, 50, 55, 67 and 75) had a more homogeneous

233   water structure for the upper 30-50 m, while stations 52 and 65, placed outside the eddy at the eastern

234   side of the sampling area, showed higher surface salinity values and the deepest UML (more than 70 m).

235

236   *3.2 Particulate organic matter*

237   The concentration and distribution of chlorophyll-a in the three areas (Table 3) varied, depending on the

238   physical constraints. In ROME 1 the stations characterised by early ice melting showed deeper mixed layers

239   and rather homogeneous chlorophyll-a concentrations in the UML, ranging from 1 to 2 µg l^{-1}. On the other

240   hand, where the alocline was shallower and the stratification stronger (i.e. station 16), a subsurface

241   increase in concentration up to 3 µg l^{-1}was observed, leading to higher average values (Table 3).

242   The chlorophyll-a distribution in ROME 2 was influenced by the previously described hydrological front,

243   associated with the deepening of the thermocline at stations 34 and 45. The frontal structure and the

244   current convergence allowed high chlorophyll-a concentrations at higher depths (values up to 3 µg l^{-1} at

245   100 m, data not shown).

10

246   The UML at stations 55, 67 and 75, in ROME 3, directly influenced by the cyclonic eddy, showed the highest

247   mean chlorophyll-a concentrations (Table 3), with maximum values higher than 4 μg l^{-1}.

248   The POC values correlated significantly with the chlorophyll-a ones in ROME 1 and ROME 3 (Table 4). ROME

249   2, instead, showed no significant correlation. ROME 2 was, however, significantly richer ($p < 0.05$) than the

250   other two at 50 and 100 m depths (Fig 6A).

251   The POC/chlorophyll-a ratio indicates the primary biomass contribution to the total POM, the lower the

252   value the higher the phytoplanktonic contribution (Fonda Umani et al., 2002). The ratio values (Table 3)

253   highlighted a generally lower contribution of the photoautotrophic component at the UMLs of ROME 1 and

254   2, with ratio values higher than 150. In ROME 1 the stations experiencing longer ice-free conditions

255   (stations 9 and 11, for instance) showed the highest ratio values in the entire mixed layer, and station 52 in

256   ROME 3 also showed the same features. At the other stations in ROME 1 and 2 the ratio decreased with

257   depth, reaching its lowest values (ratio near 50) at station 34. In ROME 3 the lowest ratio values were,

258   instead, found in both the surface and subsurface layers, especially for the stations lying to the west of the

259   frontal zone.

260   Although the PN and POC concentrations were strongly correlated (Table 4), indicating similar distributions

261   (Figs. 6A and 6B) and, possibly, origin, the POC/PN ratio values showed variations with depth (Fig 6C). The

262   POC/PN ratio gives an estimate of the N contribution to the bulk POM, keeping in mind that N-containing

263   molecules are considered attractive to consumers (Huston and Deming, 2002). The highest POC/PN ratio

264   values (above 8) were found in the deeper water layers, especially at stations 9 and 11 in ROME 1 and 50,

265   52, 56, 69 and 75 in ROME 3. The lowest values, below 6, were, instead, found in the UML, especially in

266   ROME 3, where the highest chlorophyll-a values were found. However, significant chlorophyll-a and

267   POC/PN ratio correlations were only found in ROME 2, although this relationship ($r = 0.48$, $n = 19$, $p < 0.05$)

268   highlighted that an increase of autotrophic biomass led to a lowering of the trophic value of the POM.

269   On average, the protein and carbohydrate concentrations showed vertical trends very similar to the POC

270   ones (Figs. 6D and 6G). This was also confirmed by the significant correlations found between these

271   variables for the three areas (Table 3). Proteins and carbohydrates correlated also with chlorophyll-a in

272   ROME 1 and 3, while no significant correlation was found in ROME 2. Furthermore, the hydrolysable

273   fraction of the carbohydrates and lipids was not coupled with the other variables in ROME 2 and a

274   reduction of the hydrolysable carbohydrates was, in fact, observed starting from 100 m (Fig. 6H). In this

275   area the lipid concentrations (Fig. 6I) did not show significant decreases with depth (UML vs. deeper layer,

276    $p>0.05$) but rather similar values, significantly lower than in the other areas ($p<0.001$).

277   On average, the hydrolysable proteins were 35.4±11.7% of the total proteins (ranging from 6.8 to 75.6%),

278   the hydrolysable carbohydrates 13.1±10.8% of the total carbohydrates (ranging from 0.1 to 44.9%).

279   Generally the deeper layer percentages were higher than the UML ones, except for the front-related

280   stations in ROME 2 and station 20 in ROME 1. This was also true considering the sum of the contribution of

281   hydrolysable proteins and carbohydrates to the POC (Fig 7).

282

283   *3.3 Multivariate statistical analysis*

284   Fig. 8 reports the PCA plot, where the cluster analysis results are shown as ellipses defined by Euclidean

285   distances. The PC1 axis explained 71% of the variation, while the PC2 explained a further 24% of the

286   variation. Two significantly different main groups (ANOSIM analysis, Table 5) were observed: the UML

287   observations belonged to the richer group A, with the exception of the closed-pack, the early summer

288   polynya observations, station 20 of ROME 1 and station 34 of ROME 2. Those observations were grouped

289   together with all the deeper-layer observations in group B. Proteins and carbohydrates explained the major

290   part of this difference (SIMPER analysis, Table 5). The group B stations showed POC concentrations 3.4-fold

291   lower than the observations of group A, 4.8 for proteins and 2.8 for carbohydrates.

292   In group A the samples were organised into two main sub-groups: a1 and a2. The multivariate analyses

293   highlighted significant differences between these sub-groups (ANOSIM analysis, Table 5), mainly due to the

294   different ratios between proteins and carbohydrates (explaining 41% of the difference, SIMPER analysis,

295   Table 5). In group B two more sub-groups were recorded, differing significantly (ANOSIM analysis, Table 5)

296   due to the carbohydrate concentrations (explaining 47% of the difference, SIMPER analysis, Table 5).

297 Each sub-group had a particular signature, defined by the previous studies carried out in the area (Table 2):

298 sub-group a1 clustered the MIZ stations (8, 10, 28, 30) and the spring polynya station MP, sub-group a2 the

299 coastal TNB stations. The surface observations characterised by a closed-pack coverage (27 and 29)

300 belonged to sub-group b1, together with the main part of the deeper layer observations; sub-group b2

301 collected those of the early summer polynya stations (15, 17, 19, 21) and the deeper coastal layer

302 observations (TNB).

303

304 *3.4 Caloric value analysis*

305 The caloric value of the POM in the two water layers was only calculated for those stations where the lipid

306 analysis was carried out, namely 9, 13, 16 and 20 of ROME 1, 34, 39 and 45 of ROME 2 and 50, 55 and 67 of

307 ROME 3. The plot of these results, with the previous research carried out in the Ross Sea and at the coastal

308 TNB (Table 2) is presented in Fig. 9. In this figure we have merged the bulk quantitative (POC) and

309 qualitative (caloric value) information on the POM.

310 Previous research highlighted a rising trend of the quantitative features in the UML, from the poorer pack-

311 ice zones to the polynya and then to the MIZ, ending with the richer coastal sites, although the MIZ could

312 also show high concentrations of POM of moderate caloric values. The previous pack-ice observations

313 showed that low concentrations were associated with an average caloric value, especially at the northern

314 station 27, while the qualitative value of the other stations was higher (MIZ and coastal) or lower (polynya).

315 The observations of the deeper layer of the MIZ and of the spring-early summer polynya showed similar

316 features to areas influenced by pack-ice, while the coastal observations had higher quantitative and

317 qualitative characteristics.

318 The stations in ROME 2 matched the quantitative and qualitative features of the polynya in the entire water

319 column. The surface observations of the other areas were grouped with the MIZ and previous coastal

320 observations for the UML. The deeper layer observations in the ROME 1 and ROME 3 areas resembled

321 those of the MIZ, spring polynya and deeper pack-layer, although their caloric value was higher.

322

13

4. Discussion

4.1 Quantitative and qualitative trophic features of the summer POM: a comparison with previous studies in the Ross Sea

The study of the features and role of the POM in the ecosystem may be approached at different levels. The first level we tested was focused on the quantitative characteristics of the stations (PCA multivariate analysis, Fig. 8). Although the UML was rather thin at several stations, significant quantitative differences were observed between the two water layers (Table 5), with a sharp reduction in POM in the deeper layer, already established by the observations by Nelson (1996), Fabiano et al. (2000) and Gardner et al. (2000) for the Ross Sea. They stated that the primary production is recycled in the photic layer and only a small part (less than 20%) will sink to the bottom, following the concept of a "retentive system". The grouping of the observations of the two layers, as revealed by the multivariate analysis, indicated a stronger and significant variability in the UML, while the deeper layer was rather homogeneous, also when compared to observations from other years and seasons.

Except for the northern stations of ROME 1 (18 and 20), ice-free water conditions were established in the whole ROME sampling area starting from the beginning of January, at least two weeks before the sampling. Open water conditions, resembling those of the previous spring-summer polynya/open water observations used as a comparison (Table 2), should then be common. The multivariate analysis indicated polynya/open-water features for the UML, but many were also similar to the previous MIZ observations.

The sub-group a1 linked some stations of the ROME cruise and the previously studied spring polynya station MP. Nevertheless, Fabiano et al. (2000) observed that this station was part of a more complex period of melting-ice. This may explain why this station was also grouped with the spring MIZ ones in the PCA plot. The MIZ stations were generally characterised by high POM productivity (Saggiomo et al., 1998; Fitch and Moore, 2007), being the priming for further planktonic development. The multivariate statistical analysis indicated that these stations showed rather high POM concentrations and, in particular, the highest prevalence of proteins over carbohydrates. It is well known that N-rich proteins cover multiple roles (energy, functional, plastic) and thus they are proxies of good trophic value POM (Etcheber et al., 1999).

14

349   Particulate carbohydrates, instead, generally have a lower trophic quality, because they are composed by

350   complex structural polysaccharides whose digestion is highly energy-consuming. One of the main processes

351   that enrich the POM of proteins is microbial activity. Microbial heterotrophic reworking of autotrophic and

352   detrital POM, generally performed by bacteria, increases the N content of the detritus (Povero et al., 2003)

353   and of the autotrophic colonies (Carlson et al., 1998) especially during summer. A general and marked

354   dominance of proteolysis over other classes of hydrolytic enzymes has been previously reported (Misic et

355   al., 2002; Celussi et al., 2009), indicating an efficient N-recycling by unicellular heterotrophs. The conversion

356   of detrital-N into high trophic value biomass is completed by an efficient microbial-loop, recovering a large

357   part of the DOM released during phytoplanktonic blooming (Kirchman et al., 2001). In addition, Sala et al.

358   (2005) found that bacteria might utilise other DOM sources (in particular dissolved carbohydrates), thus

359   increasing their efficiency in biomass accumulation.

360   Another process that may increase the protein concentration is the blooming of phytoplankton with a high

361   constitutive protein content. For instance, in cold waters the diatom protein content is approximately

362   double that of temperate waters, which results in a low POC/PN of approximately 5 (Young et al., 2015).

363   The very high chlorophyll-a concentrations of some of these stations (48, 56 and 75 for instance) agree with

364   this second hypothesis and bring these stations closer to the highly productive spring season.

365   The other UML observations of the ROME cruise (sub-group a2) resembled the coastal features of TNB

366   during summer, showing the highest concentrations of POM, although their trophic quality was lower than

367   that of sub-group a1.

368   These concentrations may depend on heterotrophic as well autotrophic activity. For instance, the long-

369   term ice-free stations of ROME 1 (9 and 11) showed a heterotrophic signature (high POC/chlorophyll-a ratio

370   values), indicating the relaxing of the primary production or an overwhelming activity of metazoans that

371   prevented the accumulation of the autotrophic biomass. Grazers and predators would take up the POM

372   resources and release trophically-depleted residuals, as indicated by the POC/PN ratio values of

373   approximately 8 in the deeper layer of these stations, and as observed by Huston and Deming in the Arctic

374   (2002).

In the Ross Sea the autotrophic processes occurring during summer could provide a large accumulation of biomass, strongly sustaining the ecosystem. This feature was not clear in the multi-year comparison by Arrigo and van Djiken (2004) and in the studies by Smith and Asper (2001) and Rigual-Hernandez et al. (2015), who observed a general decrease of chlorophyll-a concentrations from spring to summer in normal years.

The study of the ROME 3 results may help to explain the reasons for these highly productive features. The results obtained during this cruise provided a good example of the relationships between physical forcing, phytoplanktonic biomass and POM accumulation. In this case the UML depth (generally deeper than 30 m) exerted a lower influence on the POM production and accumulation than that observed by Fragoso and Smith (2012), who noted that the shallower mixed layer depths (<20 m) in late spring and early summer appeared to promote diatom growth. The phytoplanktonic biomass was absolutely pivotal for the POM composition. In fact, it regulated the POM quantitative features, as revealed by the highly significant correlations between the chlorophyll-a and the quantitative variables of the POM (Table 4) (Davis and Benner, 2005) and by the POC/chlorophyll-a ratio values for the stations on the western side of the area (eddy-influenced zone), that were significantly lower ($p < 0.05$) than the other ROME areas. Young et al. (2015) found that Antarctic diatoms should devote up to 50% of biomass to protein, explaining the very high significance of the correlation. Arrigo and van Djiken (2004) described the area of ROME 3 as a boundary between spring blooms and summer blooms. A sort of frontal area, that may show an unusually high chlorophyll-a accumulation at the surface, depending on general atmospheric conditions over the entire Ross Sea. The blooming we observed was influenced by the peculiar physical constraints of this area, such as the presence of a frontal area and a cyclonic eddy that divided some of the richer north-western stations from the others. The water mixing of the UML, due to the more intense hydrodynamic forcing, fertilised the surface layer, probably stripped of nutrients by earlier spring blooms. On the other hand, a higher instability in the water column, that is known to influence phytoplanktonic development, could have favoured some species that, before, were limited by competition (Fonda Umani et al., 2002).

400   The last sub-group showing polynya features is the b2 of the PCA. In this group station 20 of ROME 1

401   matched the features of the early summer polynya stations, despite the fact that it was ice-free for a

402   shorter time than the others. Horizontal advection of POM from the adjacent areas could have provided

403   the concentrations we found (Rigual-Hernández et al., 2015). The heavier ice-influence could have favoured

404   the accumulation and persistence of sympagic-derived materials, as indicated by the rather high surface

405   chlorophyll-a concentrations.

406

407   *4.2 Caloric value of summer POM*

408   The plotting of the POC with the POM caloric value (Fig. 9) provides information on the energy potentially

409   provided to heterotrophic consumers by the POM.

410   The ROME stations that qualitatively resemble the spring and early-summer features of the polynya were

411   those of ROME 2. Actually, these stations experienced real polynya environmental conditions, being next to

412   the TNB polynya. The ROME 2 stations, in fact, had low caloric values in the entire water column, although,

413   from a quantitative point of view, some of them in the UML had similar features to the richer coastal areas

414   (sub-group a2 of Fig 8). Low current velocities and a peculiar physical structure of the water column of

415   ROME 2 favoured subsurface summer blooming. Furthermore, the elevated pigment concentrations also

416   extended deeper in the water column, indicating that phytoplanktonic colonies were slowly sinking in the

417   relatively non-turbulent water. This physical quietude allowed the POM to sink while maintaining the same

418   caloric content of the mixed layer, as previously found for the coastal TNB (Fabiano et al., 1996), when the

419   caloric value was on average 5.33 Kcal/g. Actually, this is not very high, due to the high contribution of

420   carbohydrates that have the lowest caloric value among the three biochemical components. We observed

421   that in ROME 2 the chlorophyll-a was associated with carbonaceous POM (it correlated positively to the

422   POC/PN ratio), therefore in this area the freshly-produced summer POM had different features, namely a

423   lower trophic value, than the offshore area.

424

425   *4.3 Hydrolysable proteins and carbohydrates of summer POM*

426 Generally, the hydrolysable protein contribution was rather low during the ROME cruise, on average 35% of

427 the total proteins. This value was clearly lower than the contribution (higher than 90%) observed at coastal

428 stations in the NW Mediterranean (Misic and Covazzi Harriague, 2008), and by Fabiano and Pusceddu

429 (1998), who observed that 60% of the total proteins in TNB were hydrolysable. Anyway, these differences

430 may be due to the fact that the cited authors used trypsin to hydrolyse proteins, while in the present study

431 we used proteinase K.

432 The contribution of the hydrolysable fraction to the POC highlighted slight but interesting differences

433 between the ROME areas and also within the same area, following the mesoscale physical features.

434 Assuming that the POM production in the Ross Sea has a main phytoplanktonic signature (Fragoso and

435 Smith, 2012), the fresh (generally more labile) POM should be found at the surface at the beginning of the

436 productive season (spring), but the POM vertical fluxes of summer and the proliferation of the bacterial

437 biomass would provide sinking particles of labile heterotrophic materials such as proteins.

438 At the ROME sites the contribution of the labile proteinaceous C to the POC and the N to the TN were,

439 generally, higher in the deeper layer than in the mixed layer (Fig. 7, related also to the hydrolysable

440 carbohydrates). In ROME 1 this was particularly true for the stations that had experienced longer ice-free

441 conditions. Generally, in ice-free areas, the relaxing of the stratification due to wind and waves allows an

442 increased vertical flux of POM in terms of quantity and also of velocity of the sinking (Hargrave et al., 2002).

443 The lower maturity of station 20 (namely a higher ice-influence as revealed by salinity), instead, led to

444 conditions more similar to spring, with a higher labile contribution at the surface.

445 ROME 2, instead, showed peculiar features. Despite being ice-free for the longest time and lying nex to the

446 winter polynya of TNB, its stations showed a lower labile contribution in the deeper layer than in the UML.

447 Station 39 was the exception, lying to the east of the hydrological front and being influenced by an offshore

448 current coming from the ROME 1 area. The other stations were separated from the actual offshore area by

449 the front found at stations 34 and 45.

450 The vertical transport of the POM has a double relevance: it is essential for the foraging of bottom and

451 mesopelagic communities, and it may contribute to the CO_2 biological pump. The occurrence of vertical

452 transport, as shown by the ROME 2 and coastal observations in terms of bulk POM, may improve deep sea

453 trophism, but also push C into the deep current system via bottom-water. The vertical distribution of POM

454 at the ROME 2 stations was encouraging, because the POM accumulation was observed down to 200 m. In

455 fact, the TNB area is characterised by the formation of dense water masses due to brine release during sea-

456 ice roduction (HSSW) and by the freshening and cooling of the HSSW due to contact with the ice shelf

457 (TISW). HSSW fills-up the deeper layer of the Drygalsky Basin and flows northwards until it reaches the

458 shelf-break, where overflows down the continental slope, ventilating to the abyssal depths near Cape

459 Adare (Jacobs et al., 1970; Withworth and Orsi, 2006; Budillon et al., 2011).

460 The deep layer POM of ROME 2 was more refractory, showing proportionally lower hydrolysable proteins

461 and carbohydrates, higher POC/PN ratio, lower protein/carbohydrate ratio and a lower caloric content than

462 the mixed layer. If refractivity is a limiting factors for the biological respiration of POM, it allows a more

463 efficient burial of unrespired C to the depth, indicating TNB as a sink for C in summer (Fonda Umani et al.,

464 2002).

465

466 **5. Conclusions**

467 In this study we firstly aimed at determining whether the POM was uniformly distributed in the Ross Sea

468 during a particular season (summer), when one of the main constraints regulating POM production and

469 consumption (namely the ice cover) was generally lacking. We found that heterogeneity was still a

470 dominant feature of the Ross Sea, due to the mesoscale characteristics of each area. The presence of fronts

471 and eddies, with high current intensities, mixed the UML, stimulating phytoplanktonic production and POM

472 accumulation. Nevertheless, the vertical and horizontal extent of this fertilisation was not continuous. The

473 offshore ROME 1 and 3 areas differed from the ROME 2 area, especially with regards to the qualitative

474 trophic features of the POM. The deeper-layer POM was found to have higher lability in ROME 1 and 3,

475 while the more coastal ROME 2 had inverse features. This may be relevant, because the POM of the deeper

476 water, which would likely join the dense-water journey to the abyssal depths of the oceans, has a

477 potentially lower trophic value and could be respired to a lesser extent, contributing to C sinking to the

478 bottom. On the other hand, enrichment of the deeper POM of the other areas via bacterial growth and high

479 protein-containing phytoplankton would increase its trophic value, providing a valuable source of materials

480 and energy for those consumers that also maintain a certain metabolic activity during winter.

481 This study also highlighted that the heterogeneity of the offshore areas was principally a matter of the

482 UML. This is a critical point, because the surface layer is the first to be influenced by climatic changes. Small

483 atmospheric changes could lead to increased ecological changes, altering the fragile balance of the

484 Southern Ocean.

485

493

494 **References**

495 Arrigo, K.R., Worthen, D., Schnell, A., Lizotte, M.P., 1998. Primary production in Southern Ocean Waters. J.

496   Geophys. Res. 103, 15587–15600.

497 Arrigo, K.R., van Djiken, G.L., 2004. Annual changes in sea-ice, chlorophyll a, and primary production in the

498   Ross Sea, Antarctica. Deep Sea Res. I 51, 117–138.

499 Bligh, E.G., Dyer, W.J., 1959. A rapid method of total lipid extraction and purification. Can. J. Biochem.

500   Physiol. 37, 911–917.

501 Budillon, G., Spezie, G., 2000. Thermohaline structure and variability in the Terra Nova Bay polynya, Ross

502   Sea. Antarct. Sci. 12, 493–508.

503 Budillon, G., Castagno, P., Aliani, S., Spezie, G., Padman, L., 2011. Thermohaline variability and Antarctic

504   bottom water formation at the Ross Sea shelf break. Deep Sea Res. Part I, 1002–1018.

505 Budillon, G., Pacciaroni, M., Cozzi, S., Rivaro, P., Catalano, G., Ianni, C., Cantoni, C., 2003. An optimum

506   multiparameter mixing analysis of the shelf waters in the Ross Sea. Antarct. Sci. 15,105-118.

507 Carlson, C.A., Ducklow, H.W., Hansell, D.A., Smith, W.O., 1998. Organic carbon partitioning during spring

508   phytoplankton blooms in the Ross Sea polynya and the Sargasso Sea. Limnol Oceanogr. 43 (3), 275-

509   386.

510 Catalano, G., Povero, P., Fabiano, M., Benedetti, F., Goffart, A., 1997. Nutrient utilisation and particulate

511   organic matter changes during summer in the upper mixed layer (Ross Sea, Antarctica). Deep-Sea

512   Res. I 44, 97–112

513 Celussi, M., Cataletto, B., Fonda Umani, S., Del Negro, P., 2009. Depth profiles of bacterioplankton

514   assemblages and their activities in the Ross Sea. Deep-Sea Res. I 56, 2193–2205.

515 Comiso, J.C., McClain, C.R., Sullivan, C.W., Ryan, J.P., Leonard, C.L., 1993. Coastal Zone Color Scanner

516   pigment concentrations in the Southern Ocean and relationships to geophysical surface features. J.

517   Geophys. Res. 98, 2419-2451.

518 Dall, W., Moriarty, D.J.W., 1983. Functional aspects of nutrition and digestion. In: Mantel, L.H. (Ed.), The

519   Biology of Crustacea, vol. 5. Academic Press, New York, pp. 215–261.

520 Davis, J., Benner, R., 2005. Seasonal trends in the abundance, composition and bioavailability of particulate

521   and dissolved organic matter in the Chukchi/Beaufort Seas and western Canada Basin. Deep-Sea Res.

522   II 52, 3396–3410.

523 Dell'Anno, A., Fabiano, M., Mei, M.L., Danovaro, R., 2000. Enzymatically hydrolysed protein and

524   carbohydrate pools in deep-sea sediments: estimates of the potentially bioavailable fraction and

525   methodological considerations. Mar. Ecol. Progr. Ser. 196, 15–23.

526 Dubois, M., Gilles, K.A., Hamilton, J.K., Rebers, P.A., Smith, F., 1956. Colorimetric method for determination

527   of sugars and related substances. Anal. Chem. 39, 350-356.

528 Dunbar, R.B., Leventer, A.R., Mucciarone, D.A., 1998. Water column sediment fluxes in the Ross Sea,

529   Antarctica: atmospheric and sea ice forcing. J. Geophys. Res. 103 (30), 741-759.

Erofeeva, S.Y., Egbert, G.D., Padman L., 2005: Assimilation of ship-mounted ADCP data for barotropic tides: Application to the Ross Sea, J. Atmos. Oceanic Technol., 22: 721-734.

Etcheber, H., Relexans, J.-C., Beliard, M., Weber, O., Buscail, R., Heussner, S., 1999. Distribution and quality of sedimentary organic matter on the Aquitanian margin (Bay of Biscay). Deep-Sea Res. 46, 2249-2288.

Fabiano, M., Pusceddu A., 1998. Total and hydrolizable particulate organic matter (carbohydrates, proteins and lipids) at a coastal station in Terra Nova Bay (Ross Sea, Antarctica). Polar Biol. 19,125-132.

Fabiano, M., Povero, P., Danovaro, R., 1993. Distribution and composition of particulate organic matter in the Ross Sea (Antarctica). Polar Biol.13, 525–533.

Fabiano, M., Danovaro, R., Crisafi, E., La Ferla, R., Povero, P., Acosta-Pomar, L., 1995. Particulate matter composition and bacterial distribution in Terra Nova Bay (Antarctica) during summer 1989-1990. Polar Biol. 15, 393-400.

Fabiano, M., Povero, P., Danovaro, R., 1996. Particulate organic matter composition in Terra Nova Bay (Ross Sea, Antarctica) during summer 1990. Antarct. Sci. 8, 7–13.

Fabiano, M., Chiantore, M., Povero, P., Cattaneo-Vietti, R., Pusceddu, A., Misic, C., Albertelli, G., 1997. Short-term variation in particulate matter flux in Terra Nova Bay, Ross Sea. Antarct. Sci. 9, 143-149.

Fabiano, M., Povero, P., Misic, C. 2000. Spatial and temporal distribution of particulate organic matter in the Ross Sea. In Faranda, F.M., Guglielmo, L., Ianora, A. (Eds.) Ross Sea ecology. Berlin: Springer, pp. 135–150.

Fitch, D. T., Moore, J. K., 2007. Wind speed influence on phytoplankton bloom dynamics in the Southern Ocean Marginal Ice Zone, J. Geophys. Res. 112, C08006, doi:10.1029/2006JC004061.

Fonda Umani, S., Accornero, A., Budillon, G., Capello, M., Tucci, S., Cabrini, M., Del Negro, P., Monti, M., De Vittor, C., 2002. Particulate matter and plankton dynamics in the Ross Sea Polynya of Terra Nova Bay during the austral summer 1997/1998. J. Mar. Syst. 36, 29–49.

Fragoso, G.M., Smith Jr., W.O., 2012. Influence of hydrography on phytoplankton distribution in the Amundsen and Ross Seas, Antarctica. J. Mar. Syst. 89, 19–29.

556 Gardner, W.D., Richardson, M.J., Smith Jr., W.O., 2000. Seasonal patterns of water column particulate

557   organic carbon and fluxes in the Ross Sea, Antarctica. Deep-Sea Res. 47, 3423-3449.

558 Garrity, C., Ramseier, R.O., Peinert, R., Kern, S., Fischer, G., 2005. Water column particulate organic carbon

559   modeled fluxes in the ice-frequented Southern Ocean. J. Mar. Syst. 56, 133– 149.

560 Gordon Jr., D.C., 1970. Some studies on the distribution and composition of particulate organic carbon in

561   the North Atlantic Ocean. Deep-Sea Res. 17, 233–243.

562 Holm-Hansen, O., Lorenzen, C.J., Holmes, R.W., Strickland, J.D.H., 1965. FluoROMEtric determination of

563   chlorophyll. J. Cons. Perm. Int. Explor. Mer. 30, 3-15.

564 Mayer, L.M., Schick, L.L., Sawyer, T., Plante, C.J., Jumars, P.A., Self, R.L., 1995. Bioavailable amino acids in

565   sediments: a biomimetic, kinetics, based approach. Limnol. Oceanogr. 40, 511–520.

566 Nelson, D.M., Demaster, D.J., Dunbar, R.B., Smith Jr., W.O., 1996. Cycling of organic carbon and biogenic

567   silica in the Southern Ocean: estimates of water-column and sedimentary fluxes on the Ross Sea

568   continental shelf. J. Geophys. Res. 10, 18519–18532.

569 Hargrave, B.T., Walsh, I.D., Murray, D.W., 2002. Seasonal and spatial patterns in mass and organic matter

570   sedimentation in the North Water. Deep-Sea Res. II 49, 5227-5244.

571 Hartree, E.F., 1972. Determination of proteins: a modification of the Lowry method that gives a linear

572   photometric response. Anal. Biochem. 48, 422–427.

573 Hedges, J.I., Stern, J.H., 1984. Carbon and nitrogen determination of carbonate-containing solids. Limnol.

574   Oceanogr. 29, 657–663.

575 Huston, A.L., Deming, J.W., 2002. Relationships between microbial extracellular enzymatic activity and

576   suspended and sinking particulate organic matter: seasonal transformations in the North Water.

577   Deep-Sea Res. II 49, 5211–5225.

578 Jacobs, S.S., Amos, A.F., Bruchhausen, P.M., 1970. Ross Sea oceanography and Antarctic Bottom Water

579   formation. Deep-Sea Res. 17, 935–962.

580   Kim, B.K., Lee, J.H., Yun, M.S., Joo, H.T., Song, H.J., Yang, E.J., Chung, K.H., Kang, S.-H., Lee, S.H., 2014. High

581   lipid composition of particulate organic matter in the northern Chukchi Sea, 2011. Deep- Sea Res. II,

582   120, 72-81. DOI: 10.1016/j.dsr2.2014.03.022i

583   Kirchman, D.L., Meon, B., Ducklow, H.W., Carlson, C.A., Hansell, D.A., Steward, G.F., 2001. Glucose fluxes

584   and concentrations of dissolved combined neutral sugars (polysaccharides) in the Ross Sea and Polar

585   Front Zone, Antarctica. Deep-Sea Res. II 48, 4179–4197.

586   Marsh, J.B., Weinstein, D.B., 1966. A simple charring method for determination of lipids. J. Lipid Res. 7, 574-

587   576.

588   Mayer, L.M., Schick, L.L., Sawyer, T., Plante, C.J., Jumars, P.A., Self, R.L., 1995. Bioavailable amino acids in

589   sediments: a biomimetic, kinetics, based approach. Limnol. Oceanogr. 40, 511–520.

590   Misic, C., Covazzi Harriague, A., 2008. Organic matter recycling in a shallow coastal zone (NW

591   Mediterranean): the influence of local and global climatic forcing and organic matter lability on

592   hydrolytic enzyme activity. Cont. Shelf Res. 28, 2725-2735.

593   Misic, C., Fabiano, M., 1996. A functional approach to the assessment of the nutritional value of the

594   particulate organic matter. Chem. Ecol. 13, 51–63.

595   Misic, C., Povero, P., Fabiano, M., 2002. Ectoenzymatic ratios in relation to particulate organic matter

596   distribution (Ross Sea, Antarctica). Microb. Ecol. 44, 224–234.

597   Orsi, A.H., Wiederwohl, C.L., A recount of Ross Sea waters. Deep-Sea Research II (2009), doi:10.1016/

598   j.dsr2.2008.10.033

599   Povero, P., Chiantore, M., Misic, C., Budillon, G., Cattaneo-Vietti, R., 2001. Land forcing controls pelagic-

600   benthic coupling in Adélie Cove (Terra Nova Bay, Ross Sea). Polar Biol. 24, 875–882.

601   Povero, P., Misic, C., Ossola, C., Castellano, M., Fabiano, M., 2003. The trophic role and ecological

602   implications of oval faecal pellets in Terra Nova Bay (Ross Sea). Polar Biol. 26, 302–310.

603   Rigual-Hernández, A.S., Trull, T.W., Bray, S.G., Closset, I., Armand, L.K., 2015. Seasonal dynamics in diatom

604   and particulate export fluxes to the deep sea in the Australian sector of the southern Antarctic Zone.

605   J. Mar. Syst. 142, 62–74.

606 Rivaro, P., Messa, R., Ianni, C., Magi, E., Budillon, G., 2014. Distribution of total alkalinity and pH in the Ross

607 Sea (Antarctica) waters during austral summer 2008. Polar Research 33,

608 20403,http://dx.doi.org/10.3402/polar.v33.20403.

609 Rivaro, P., Ianni, C., Langone, L., Ori, C., Aulicino, G., Cotroneo, Y., Saggiomo, M., Mangoni O., this issue.

610 Physical and biological forcing on the mesoscale variability of the carbonate system in the Ross Sea

611 (Antarctica) during the summer season 2014. J. Mar. Syst., in press.

612 Saggiomo, V., Carrada, G.C., Mangoni,O., Ribera d'Alcalà, M., Russo A., 1998. Spatial and temporal

613 variability of size-fractionated biomass and primary production in the Ross Sea (Antarctica) during

614 austral spring and summer. J Mar. Syst. 17, 115–127.

615 Sala, M.M., Arin, L., Balagué, V., Felipe, J., Guadayol, Ò., Vaqué, D., 2005. Functional diversity of

616 bacterioplankton assemblages in western Antarctic seawaters during late spring. Mar. Ecol. Prog. Ser.

617 292, 13–21.

618 Smith Jr, W.O., Nelson, D.M., Di Tullio, G.R., Leventer, A.R., 1996.Temporal and spatial patterns in the Ross

619 Sea: phytoplankton biomass elemental composition, productivity and growth rates. J. Geophys. Res.

620 101, 18455–18466.

621 Smith Jr., W.O., Asper, V.A., 2001. The influence of phytoplankton assemblage composition on

622 biogeochemical characteristic and cycles in the Southern Ross Sea, Antarctica. Deep Sea Res. I 48,

623 137–161.

624 Smith Jr., W.O., Marra, J., Hiscock, M.R., Barber, R.T., 2000. The seasonal cycle of phytoplankton biomass

625 and primary productivity in the Ross Sea, Antarctica. Deep Sea Res. II 47, 3119–3140.

626 Spreen, G., L. Kaleschke, and G. Heygster(2008), Sea ice remote sensing using AMSR-E 89 GHz channels *J.*

627 *Geophys. Res.*, vol. 113, C02S03, doi:10.1029/2005JC003384.

628 Winberg, G.G., 1971. Symbols, units and conversion factors in study of fresh waters productivity. Int. Biol.

629 Programme, 23.

630 Whitworth T., III, Orsi, A.H., 2006. Antarctic Bottom Water production and export by tides in the Ross Sea,

631 Geophys. Res. Lett. 33, L12609,doi:10.1029/2006GL026357

632   Young, J.N., Goldman, J.A.L., Kranz, S.A., Tortell, P.D., Morel, F.M.M., 2015. Slow carboxylation of Rubisco

633   constrains the rate of carbon fixation during Antarctic phytoplankton blooms. New Phytol. 205, 172–

634   181. doi: 10.1111/nph.13021

Captions to figures

636

637 Fig. 1. A: Map of the stations of the ROME 1 (red dots), ROME 2 (blue dots) and ROME 3 (green dots) areas.

638 Black-circled points indicate the POM sampling stations. B: Θ/S diagram obtained from the entire available

639 dataset indicates the main water masses. Data from the three different areas (ROME 1, ROME 2 and ROME

640 3) are represented with different colours (red, blue and green, respectively).

641

642 Fig. 2. Sea-ice concentration maps of the Ross Sea for 1 December (A), 19 December (B), 7 January (C), 14

643 January (D). Red circles and numbers highlight the position of the ROME 1, ROME 2 and ROME 3 sampling

644 areas.

645

646 Fig. 3. Station map (A) and maps of mean salinity (B), temperature (C) and currents (D) in the upper mixed

647 layer at ROME 1.

648

649 Fig. 4. Station map (A) and maps of mean salinity (B), temperature (C) and currents (D) in the upper mixed

650 layer at ROME 2.

651

652 Fig. 5. Station map (A) and maps of mean salinity (B), temperature (C) and currents (D) in the upper mixed

653 layer at ROME 3.

654

655 Fig. 6. Vertical profiles of the variables averaged for each depth at each area (standard deviations are

656 reported). A: particulate organic carbon (POC), B: particulate nitrogen (PN), C: particulate organic

657 carbon/particulate nitrogen ratio (POC/PN), D: particulate proteins (PRT), E: hydrolysable particulate

658 proteins (h-PRT), F: particulate proteins/carbohydrate ratio (PRT/CHO), G: particulate carbohydrates (CHO),

659 H: hydrolysable particulate carbohydrates (h-CHO), I: particulate lipids (LIP).

660

661   Fig. 7. Average contribution of the hydrolysable fraction of proteins and carbohydrates to the POC in the

662   three areas. Standard deviations are reported. Grey: UML, black: deeper layer.

663

664   Fig. 8. PCA for the entire ROME cruise and for the previous studies in the upper mixed layer (UML, coloured

665   markers) and deeper layer (DL, blue markers). Two main groups (A and B) are composed of the four sub-

666   groups a1 and a2 (A), b1 and b2 (B). The ellipses are drawn following the results of the cluster analysis on

667   the normalised data (Euclidean distance = 1.8). See text and Table 2 for details. The vectors of the variables

668   are reported on the upper left of the plot.

669

670   Fig. 9. Plot of the POC concentration and caloric value of the POM for the upper mixed layer (A) and the

671   deeper layer (B). Black numbers and markers refer to the previous studies in the Ross Sea and coastal Terra

672   Nova Bay (TNB), red numbers and markers refer to the ROME cruise results. Coloured boxes group the

673   stations that have similar ice-related features (blue: pack-ice coverage, green: marginal ice zone – MIZ, red:

674   polynya) or belong to the coastal sites (violet). See Table 2 for details.

675   Table 1. Position of the stations sampled for POM characterisation during the ROME cruise in 2014, depth of the

676   upper mixed layer (UML) and number of sampled depths for each station.

677

	station	date	longitude (°E)	latitude (°S)	UML depth (m)	sampled depths
ROME 1	9	16 Jan	173.87	75.00	38	5
	11	16 Jan	172.03	75.00	29	5
	13	16 Jan	170.76	75.00	32	5
	16	17 Jan	169.50	74.83	15	5
	18	17 Jan	169.51	74.51	17	5
	20	17 Jan	169.88	73.99	14	5
ROME 2	33	26 Jan	166.06	74.70	18	4
	34	26 Jan	165.75	74.76	13	5
	36	27 Jan	165.18	74.88	12	5
	39	27 Jan	166.06	74.86	24	4
	43	27 Jan	164.98	74.79	14	4
	45	28 Jan	165.49	74.82	15	5
ROME 3	48	31 Jan	167.83	76.40	33	5
	50	31 Jan	168.65	76.40	36	5
	52	1 Feb	169.53	76.42	75	4
	55	1 Feb	168.40	76.43	44	5
	56	1 Feb	168.16	76.54	12	5
	65	2 Feb	169.58	76.50	115	4
	67	2 Feb	168.72	76.50	51	5
	69	2 Feb	168.01	76.50	14	4
	75	3 Feb	168.80	76.38	42	5

678

679 Table 2. Features of the stations sampled during previous researches, here used as a comparison for the ROME

680 cruise observations.

681

area	season	environmental features	station	lat °S	long °E	reference
Ross Sea		polynya	MP	76.50	175.00	
		MIZ	8	75.16	175.18	
		MIZ	10	74.84	174.88	
	spring	MIZ	28	74.70	172.01	Fabiano et al. (2000)
		MIZ	30	74.69	164.18	
		pack	27	71.94	174.98	
		pack	29	74.98	167.99	
		polynya	15	72.35	179.78	
		polynya	17	73.23	179.84	
	early summer	polynya	19	74.95	179.82	Fabiano et al. (1993);
		polynya	21	74.98	174.87	Catalano et al. (1997)
		MIZ	23	74.99	170.00	
		MIZ	25	74.95	165.25	
Terra Nova Bay			TNB	74.78	164.17	Povero et al. (2001)
	summer	coastal-open waters	TNBa	74.75	164.17	Fabiano et al. (1995)
			TNBb	74.70	164.13	Fabiano et al. (1997)

682

683   Table 3. Average data and standard deviation (sd) for the upper mixed layer (UML) and the deeper layer (DL) of the ROME 1, ROME 2 and ROME 3 stations.

position	station	water layer	Chl-a µg/l	sd	PN µg/l	sd	POC µg/l	sd	PRT µg/l	sd	h-PRT µg/l	sd	CHO µg/l	sd	h-CHO µg/l	sd	LIP µg/l	sd	POC/Chl-a	sd	POC/PN	sd	PRT/CHO	sd
ROME 1	9	UML	1.62	0.06	48.7	2.1	297.3	13.7	319.7	3.9	84.2	1.1	96.7	15.0	7.4	8.8	80.6	17.2	184.2	15.3	6.1	0.0	3.3	0.5
		DL			6.7	6.5	48.5	39.5	47.6	47.9	18.4	14.2	21.6	13.4	5.0	2.1	18.3	18.6			8.0	2.4	1.9	1.0
	11	UML	1.66	0.14	50.3	5.5	290.5	19.2	324.4	23.8	78.0	1.6	123.7	24.3					174.8	2.7	5.8	0.3	2.7	0.3
		DL			5.9	3.5	39.6	15.6	49.4	17.4	17.1	6.6	16.3	5.9							7.4	1.6	3.1	1.2
	13	UML	2.02	0.35	44.9	15.9	275.1	98.0	335.3	116.1	116.1	65.1	108.5	52.3	18.3	21.8	67.7	22.6	133.7	25.3	6.1	0.0	3.2	0.5
		DL			4.7	3.3	40.3	30.2	45.1	34.3	19.3	16.7	22.5	11.9	4.0	3.0	14.8	13.6			6.8	0.8	1.9	0.6
	16	UML	2.99	0.04	48.5	41.1	301.0	202.5	333.6	225.8	105.4	44.1	118.9	82.1	13.8	16.3	67.1	5.1	101.2	69.1	5.6	0.2	2.8	0.0
		DL			4.3	2.0	32.3	19.3	34.1	34.3	15.9	15.2	19.1	6.3	2.6	1.9	5.6	4.9			6.6	0.4	1.5	1.1
	18	UML	1.50	0.22	38.1	15.8	208.1	97.3	240.7	107.4	69.9	39.1	63.7	45.3					144.9	86.2	5.5	0.2	4.3	1.3
		DL			4.4	1.8	27.1	8.5	27.0	10.4	8.6	4.4	9.6	2.2							6.3	0.7	2.8	0.5
	20	UML	2.32	0.16	18.3	0.7	112.4	4.3	134.7	15.8	44.6	1.3	52.6	6.2	2.5	1.2	27.5	9.4	48.5	1.5	5.7	0.6	2.6	0.6
		DL			2.7	1.7	21.6	11.4	15.7	15.3	5.6	6.1	12.8	4.1	1.4	1.5	9.4	2.8			7.3	0.3	1.1	0.8
ROME 2	33	UML	1.10	0.04	34.0	5.7	192.3	36.7	226.5	63.8	76.0	18.6	87.8	42.1					174.0	27.2	5.7	0.2	2.7	0.6
		DL			11.4	4.2	70.2	25.5	63.1	28.0	24.1	9.1	23.3	7.0							6.2	0.0	2.6	0.4
	34	UML	2.63	0.10	26.9	8.7	195.0	16.9	206.0	49.7	79.1	14.2	128.0	32.3	17.9	10.4	49.3	2.6	74.4	9.2	6.5	0.4	1.7	0.8
		DL			18.7	5.9	145.5	57.1	136.7	62.6	54.4	28.0	98.6	63.0	16.8	24.4	22.0	12.9			7.4	0.7	1.5	0.4
	36	UML	2.18	0.36	36.1	2.7	212.9	20.2	242.1	2.6	77.5	6.1	68.6	3.1					117.5	64.1	5.9	0.1	3.5	0.1
		DL			16.1	11.9	129.2	92.2	95.8	61.6	29.4	17.1	54.5	40.6							8.0	0.8	1.8	0.5
	39	UML	1.00	0.06	43.1	1.1	233.5	1.2	277.3	16.7	86.7	11.9	104.2	11.8	23.5	5.0	32.5	12.1	232.9		5.4	0.1	2.7	
		DL			15.2	9.0	108.3	74.0	115.3	79.8	52.5	30.6	76.3	61.7	7.9	6.1	23.2	18.5			6.7	1.0	1.6	0.2
	43	UML	1.52	0.12	38.6	3.6	233.5	0.4	306.7	36.8	97.1	11.8	102.5	9.2					153.5		6.1	0.6	3.0	
		DL			14.3	10.5	100.0	74.2	115.5	104.5	41.1	39.3	62.9	47.8							7.0	0.1	1.7	0.3
	45	UML	1.30	0.14	33.5	0.7	200.8	4.6	259.2	16.6	102.5	6.0	109.0	21.8	3.3	0.4	14.9	3.9	154.4		6.0	0.0	2.4	
		DL			24.4	14.7	162.6	97.5	174.5	123.5	64.9	39.6	111.6	81.4	8.7	12.2	16.0	12.2			6.9	0.6	1.5	0.5
ROME 3	48	UML	3.01	0.16	46.7	5.3	248.4	19.3	304.5	4.9	84.1	5.7	69.2	21.2					82.5	1.9	5.3	0.2	4.6	1.3
		DL			4.7	2.4	31.9	15.8	28.0	13.8	9.5	4.6	9.6	1.8							6.9	0.4	2.8	0.9
	50	UML	3.04	0.09	44.6	1.4	263.4	8.8	298.3	9.3	79.9	5.5	102.5	4.3	14.5	12.1	52.6	16.4	86.8	5.5	5.9	0.4	2.9	0.0
		DL			8.7	8.5	62.1	54.6	72.8	72.2	34.5	31.2	24.4	16.5	2.8	2.2	17.5	20.5			7.8	0.9	2.7	1.3
	52	UML	1.09	0.05	26.2	5.3	160.9	11.0	183.6	22.2	57.5	3.0	49.1	7.3					148.1	3.6	6.3	1.7	3.8	0.1
		DL			2.6	0.6	23.4	1.7	23.3	1.1	9.5	2.1	6.8	0.1							9.5	1.9	3.4	0.2
	55	UML	3.16	2.19	42.1	24.6	252.7	130.7	305.0	184.3	106.9	51.0	103.8	69.3	24.3	18.5	78.4	16.6	103.7	51.6	5.8	0.1	3.3	0.9
		DL			3.6	0.7	23.8	1.2	21.0	2.7	13.6	0.9	11.9	0.9	0.3	0.0	10.5	1.1			6.0	0.2	1.8	0.4
	56	UML	2.71	1.92	45.7	9.8	245.1	65.7	332.6	75.2	91.6	21.0	64.7	30.3					109.2	53.1	5.3	0.3	5.5	1.4
		DL			10.2	11.5	57.1	53.8	75.8	87.4	24.8	30.6	17.6	15.6							6.7	1.8	3.7	1.2
	65	UML	1.10	0.00	22.7	0.1	123.9	12.6	158.4	13.9	30.2	23.7	41.0	1.2					112.2	11.0	5.5	0.6	3.9	0.2
		DL			5.8	2.8	34.4	15.5	42.3	23.6	15.7	7.9	12.1	5.0							6.0	0.2	3.4	0.6
	67	UML	3.64	0.64	45.1	14.2	254.6	77.9	327.0	79.7	95.9	11.7	94.3	42.5	6.3	5.1	70.0	26.0	68.8	10.2	5.7	0.2	3.8	1.2
		DL			4.5	0.8	35.0	8.4	33.0	12.4	13.8	3.1	18.1	7.4	2.6	0.1	15.4	0.8			6.1	0.5	1.8	0.1
	69	UML	2.14	0.12	27.6	1.9	175.2	25.0	199.6	11.3	48.1	31.8	53.4	5.7					81.8	7.1	6.3	0.4	3.7	0.2
		DL			7.9	6.9	49.5	32.7	73.1	58.3	21.6	14.2	13.6	8.4							7.3	2.3	5.0	1.2
	75	UML	4.03	1.02	51.9	14.3	286.7	76.2	366.5	94.0	90.0	10.8	85.8	37.0					70.9	1.3	5.5	0.1	4.5	0.9
		DL			4.0	1.2	27.5	2.0	22.7	9.1	8.2	6.2	6.8	1.5							7.2	1.6	3.3	0.6

684   Chl: chlorophyll-a, PN: particulate nitrogen, POC: particulate organic carbon, PRT: particulate proteins, h-PRT: hydrolysable particulate proteins, CHO: particulate
685   carbohydrates, h-CHO: hydrolysable particulate carbohydrates, LIP: lipids, POC/Chl: POC/chlorophyll-a ratio, PRT/CHO: protein/carbohydrate ratio, POC/PN: POC/PN ratio.

686 Table 4. Significant correlations between the different variables for each area investigated during the ROME

687 cruise. Underlined numbers: $p<0.05$, normal numbers: $p<0.01$, bold numbers: $p<0.001$. The number of

688 observation varied in the three Legs and depending on the variable: in ROME 1 chlorophyll-a showed 13

689 observations, hydrolysable carbohydrate and lipid 18, the other variables 28. In ROME 2 they were: 19, 12

690 and 25, respectively. In ROME 3: 25, 13 and 40, respectively. Abbreviations as in Table 2.

691

		chl	TN	POC	prt	h-PRT	CHO	h-CHO
ROME 1	TN	0.68						
	POC	0.72	**1.00**					
	prt	0.73	**0.99**	**1.00**				
	h-PRT	0.76	**0.94**	**0.95**	**0.97**			
	CHO	0.71	**0.97**	**0.98**	**0.98**	**0.94**		
	h-CHO	-	**0.76**	**0.75**	**0.77**	**0.83**	**0.82**	
	LIP	_0.63_	**0.89**	**0.92**	**0.91**	**0.90**	**0.88**	0.65
		chl	TN	POC	prt	h-PRT	CHO	h-CHO
ROME 2	TN	-						
	POC	-	**0.96**					
	prt	-	**0.97**	**0.95**				
	h-PRT	-	**0.89**	**0.90**	**0.94**			
	CHO	0.65	**0.68**	**0.81**	**0.77**	**0.79**		
	h-CHO	-	-	-	-	-	0.72	
	LIP	-	-	-	-	-	_0.53_	_0.63_
		chl	TN	POC	prt	h-PRT	CHO	h-CHO
ROME 3	TN	**0.95**						
	POC	**0.95**	**0.99**					
	prt	**0.95**	**0.99**	**0.99**				
	h-PRT	**0.86**	**0.93**	**0.94**	**0.94**			
	CHO	**0.90**	**0.93**	**0.95**	**0.94**	**0.91**		
	h-CHO	_0.64_	0.74	0.74	0.74	0.72	**0.80**	
	LIP	0.68	**0.91**	**0.91**	**0.90**	**0.90**	**0.89**	0.68

692

693   Table 5. Multivariate statistical analysis (ANOSIM and SIMPER) for the two main groups A and B of the PCA

694   (Fig. 8) and the sub-groups a1-a2 and b1-b2. Mean values ± standard deviation for each group and sub-

695   group are reported (POC, PRT and CHO: µg l^{-1}; PRT/CHO: µg µg^{-1}). Abbreviations as in Table 2.

696

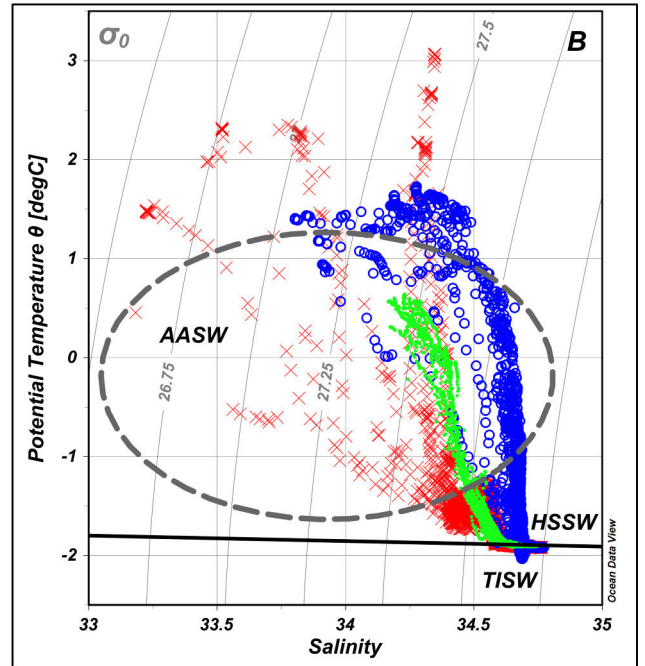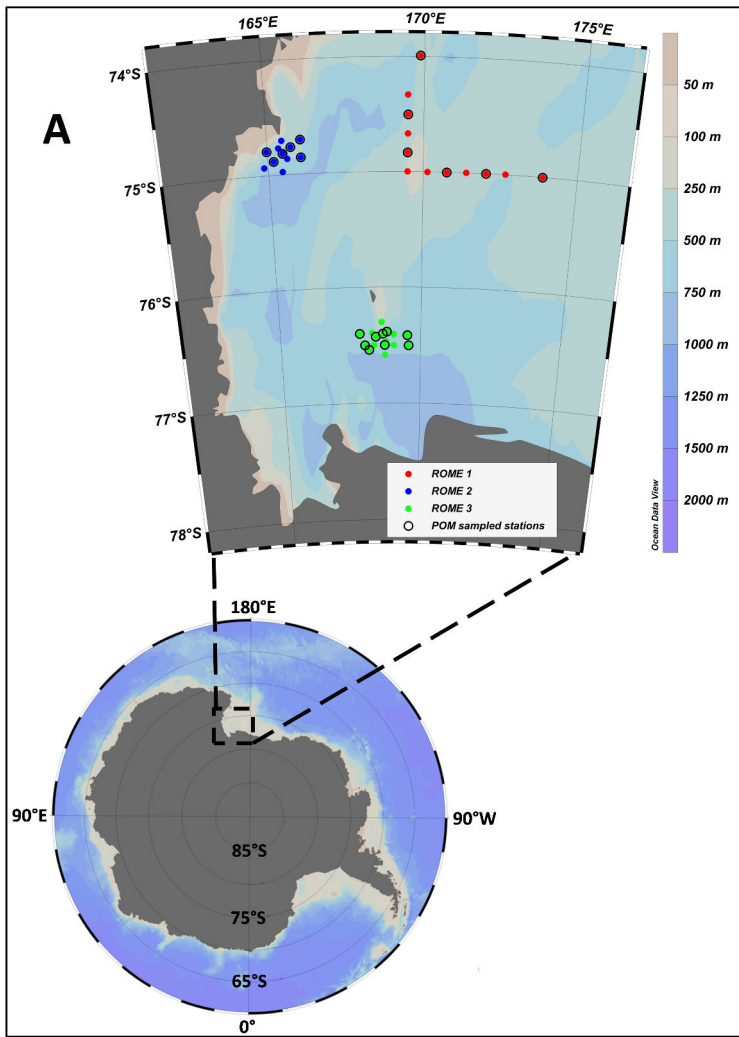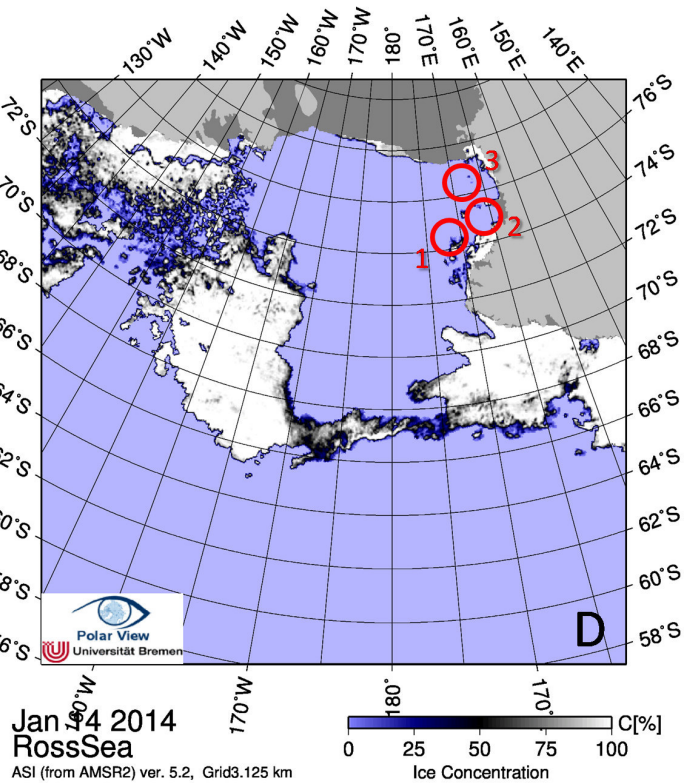| ANOSIM		
sub-groups	R statistic	significance %
A vs B	0.847	0.1
a1 vs a2	0.656	0.1
b1 vs b2	0.903	0.1

697

SIMPER						
groups	variable	%		average±sd		average±sd
A vs B	PRT	32	A:	281.4±62.9	B:	58.8±47.5
	PRT/CHO	25		3.6±1.0		2.1±0.9
	CHO	24		90.0±32.9		32.7±30.0
	POC	19		242.8±55.0		72.4±53.9
a1 vs a2	PRT/CHO	41	a1:	4.3±0.7	a2:	2.9±0.4
	CHO	36		63.1±15.7		115.1±23.0
	PRT	14		243.8±60.1		316.4±43.0
b1 vs b2	CHO	47	b1:	15.9±5.5	b2:	71.5±27.1
	PRT/CHO	22		2.2±1.0		1.7±0.4
	POC	17		40.7±14.4		145.7±36.6
	PRT	14		33.2±17.1		118.0±41.8

698

Dec 01 2013
RossSea
ASI (from AMSR2) ver. 5.2, Grid3.125 km
Ice Concentration

Dec 19 2013
RossSea
ASI (from AMSR2) ver. 5.2, Grid3.125 km
Ice Concentration

Jan 07 2014
_RossSea
ASI (from AMSR2) ver. 5.2, Grid3.125 km
Ice Concentration
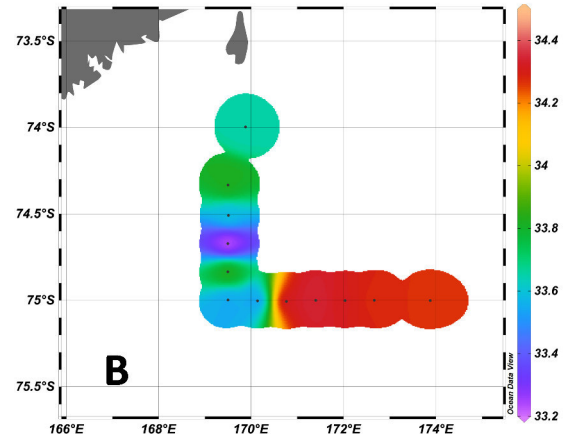
Jan 14 2014
RossSea
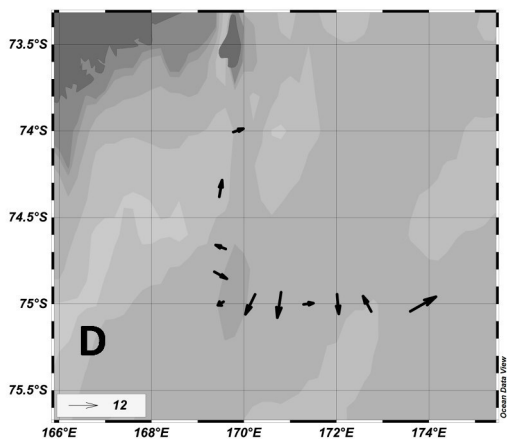ASI (from AMSR2) ver. 5.2, Grid3.125 km
Ice Concentration
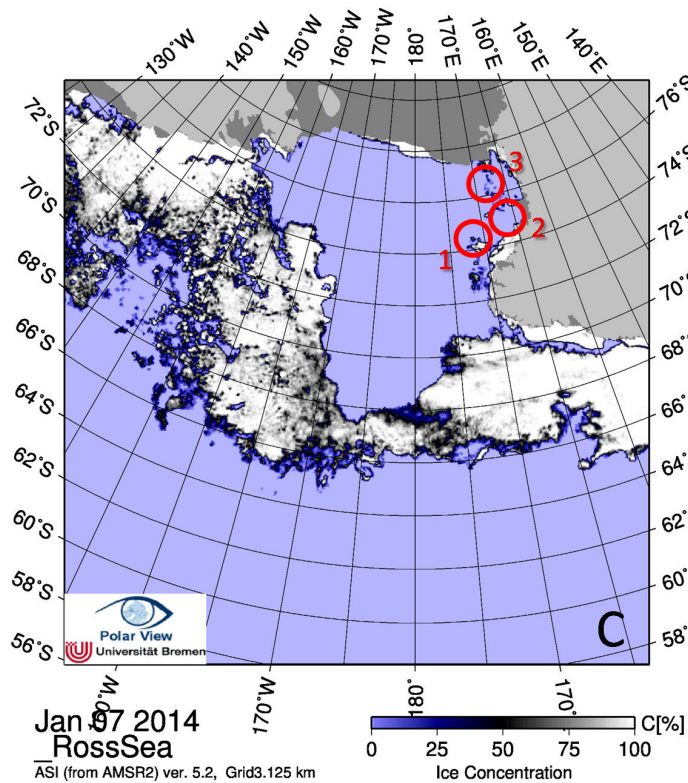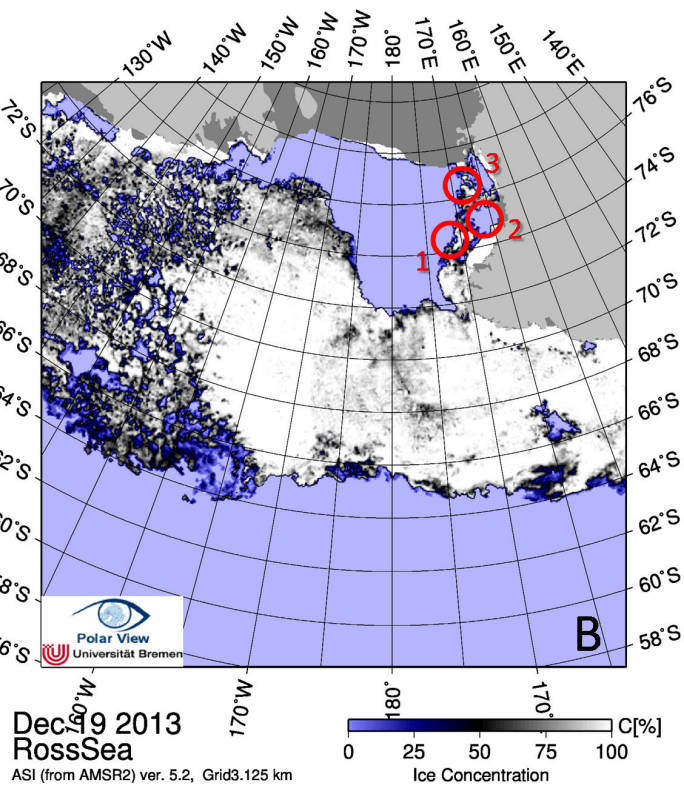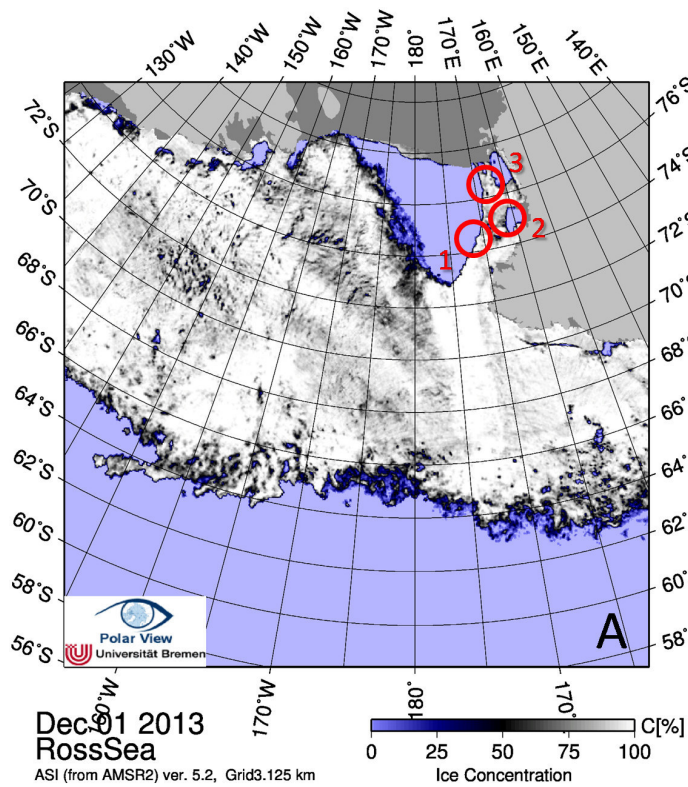
ROME 1
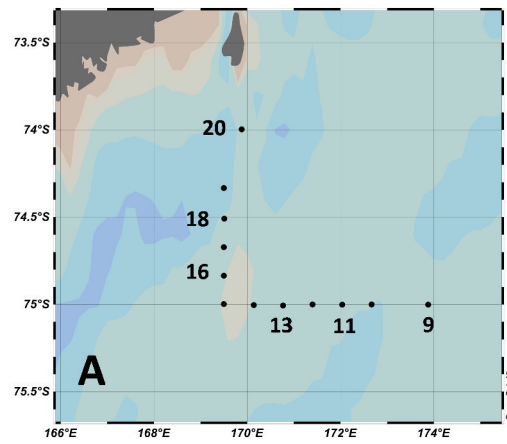
Mean salinity

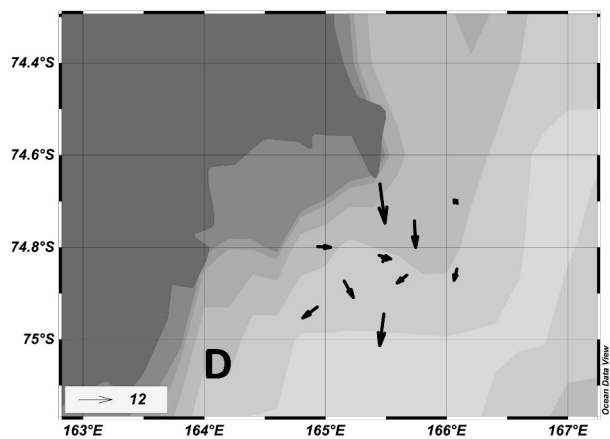**Mean currents [cm/s]**

Mean temperature [°C]

ROME 2

Mean salinity

Mean currents [cm/s]

Mean temperature [°C]

ROME 3

48 75 50 55 52 69 67 65 56

A

Mean salinity

B

Mean currents [cm/s]

Mean temperature [°C]